J Neurophysiol 122: 539–551, 2019.
First published June 12, 2019; doi:10.1152/jn.00268.2019.

RESEARCH ARTICLE | *Higher Neural Functions and Behavior*

Alpha-band oscillations track the retrieval of precise spatial representations from long-term memory

David W. Sutterer,[1,2] Joshua J. Foster,[1,2] John T. Serences,[3,4] Edward K. Vogel,[1,2] and Edward Awh[1,2]

[1]*Department of Psychology, University of Chicago, Chicago, Illinois;* [2]*Institute for Mind and Biology, University of Chicago, Chicago, Illinois;* [3]*Department of Psychology, University of California San Diego, La Jolla, California; and* [4]*Neuroscience Graduate Program, University of California San Diego, La Jolla, California*

Submitted 26 April 2019; accepted in final form 10 June 2019

Sutterer DW, Foster JJ, Serences JT, Vogel EK, Awh E. Alpha-band oscillations track the retrieval of precise spatial representations from long-term memory. *J Neurophysiol* 122: 539–551, 2019. First published June 12, 2019; doi:10.1152/jn.00268.2019.—A hallmark of episodic memory is the phenomenon of mentally reexperiencing the details of past events, and a well-established concept is that the neuronal activity that mediates encoding is reinstated at retrieval. Evidence for reinstatement has come from multiple modalities, including functional magnetic resonance imaging and electroencephalography (EEG). These EEG studies have shed light on the time course of reinstatement but have been limited to distinguishing between a few categories. The goal of this work was to use recently developed experimental and technical approaches, namely continuous report tasks and inverted encoding models, to determine which frequencies of oscillatory brain activity support the retrieval of precise spatial memories. In *experiment 1*, we establish that an inverted encoding model applied to multivariate alpha topography tracks the retrieval of precise spatial memories. In *experiment 2*, we demonstrate that the frequencies and patterns of multivariate activity at study are similar to the frequencies and patterns observed during retrieval. These findings highlight the broad potential for using encoding models to characterize long-term memory retrieval.

NEW & NOTEWORTHY Previous EEG work has shown that category-level information observed during encoding is recapitulated during memory retrieval, but studies with this time-resolved method have not demonstrated the reinstatement of feature-specific patterns of neural activity during retrieval. Here we show that EEG alpha-band activity tracks the retrieval of spatial representations from long-term memory. Moreover, we find considerable overlap between the frequencies and patterns of activity that track spatial memories during initial study and at retrieval.

alpha; EEG; inverted encoding model; memory precision; spatial memory

INTRODUCTION

The retrieval of episodic memories is defined by the phenomenon of reexperiencing the details of past events and is supported by reinstatement, the reactivation of neural activity that was present at encoding. Considerable support for this view has come from functional magnetic resonance imaging (fMRI) studies, which have shown that sensory regions involved in the initial processing of information are reengaged at retrieval (Danker and Anderson 2010; Wagner et al. 2005; Wheeler et al. 2000). Furthermore, voxelwise patterns of activity within these regions during memory retrieval resemble activity seen during encoding (Bosch et al. 2014; Hindy et al. 2016; Polyn et al. 2005; Ritchey et al. 2013). Recent work has shown that reinstatement is evident in more time-resolved measures of neural activity, such as electroencephalography (EEG) and magnetoencephalography (MEG), providing an important complement to fMRI decoding because it reveals the temporal dynamics of retrieval. However, although EEG enables temporally resolved tracking of retrieved information, it has been limited to decoding coarse information, such as the category of a retrieved paired associated or the task performed at encoding (Jafarpour et al. 2014; Johnson et al. 2015; Morton et al. 2013; Waldhauser et al. 2016; Wimber et al. 2012). Thus, it remains to be seen whether EEG activity enables temporally resolved tracking of the retrieval of precise visual feature values that are associated with specific items.

Here, we measured EEG activity during the encoding and recall of precise spatial locations from long-term memory (LTM) and applied an inverted encoding model (IEM) to the topography of oscillatory activity on the scalp. IEMs have provided a useful approach for reconstructing precise spatial representations from fMRI and EEG activity (Foster et al. 2016, 2017b; Sprague and Serences 2013; Sprague et al. 2014, 2016). Thus, we expected that IEMs might also prove an effective tool for tracking the retrieval of precise spatial memories. Critically, this approach also allowed us to test another open question: What frequency bands carry spatial information retrieved from LTM?

On the one hand, theories about the role of rhythmic oscillations in memory have proposed that the same frequencies of oscillations coordinate specific cognitive operations at encoding and retrieval (Siegel et al. 2012; Watrous and Ekstrom 2014; Watrous et al. 2015). Previous work using an IEM applied to alpha-band EEG activity, has successfully tracked covert spatial attention (Foster et al. 2017b), and spatial representations maintained in working memory (Foster et al. 2016, 2017a; Sutterer et al. 2019), which leads to the prediction that

Address for reprint requests and other correspondence: D. Sutterer, Department of Psychology, 111 21st St., Nashville, TN 37212 (e-mail: david.w.sutterer@vanderbilt.edu).

alpha-band activity should also represent spatial locations retrieved from LTM. In line with this view, alpha-band activity has been shown to track hemifield-specific memory-guided attention (Stokes et al. 2012) and memory retrieval (Waldhauser et al. 2016), and the magnitude of alpha desynchronization tracks the number of items recalled from LTM (Fukuda and Woodman 2017).

On the other hand, other frequency bands, especially theta and beta, are known to play important roles in long-term memory encoding and retrieval (Hsieh and Ranganath 2014; Kerren et al. 2018; Morton and Polyn 2017; Morton et al. 2013; Nyhus and Curran 2010) and spatial navigation (Bohbot et al. 2017; Watrous et al. 2011). Moreover, recent fMRI studies have provided evidence that the constellations of cortical regions engaged (Xiao et al. 2017) and the strength of memory representations across regions (Favila et al. 2018) are not identical during encoding and memory retrieval raising the possibility that the frequency of oscillations representing information during encoding and retrieval might also vary. Thus, we investigated which frequency bands carry spatial information retrieved from LTM.

In two experiments, participants learned to associate objects with specific angular locations. Then, they were asked to precisely report the associated location when presented with an object cue. The IEM analysis revealed that oscillatory activity tracked the precise spatial position that was retrieved from LTM. Consistent with oscillatory reinstatement accounts, we found that spatially specific patterns of activity were largely restricted to the alpha band, the same frequency band that represents spatial locations held in working memory (WM) (Foster et al. 2016; Sutterer et al. 2019). Moreover, the alpha-band patterns observed during retrieval matched those observed during the initial encoding of the objects, in line with the hypothesis that encoding-related activity was reinstated during retrieval from LTM. Finally, the selectivity of alpha-band activity tracked memory performance as learning progressed from the first to second half of the session as well as the latency with which participants reported the target locations. Together these findings suggest that LTM retrieval elicits reinstatement of the spatially specific oscillatory activity that is observed during encoding, and that multivariate analysis of alpha-band activity provides a powerful measure of the timing and success of this basic cognitive process.

MATERIALS AND METHODS

Participants. Sixty-nine adults (33 in *experiment 1*, and 36 in *experiment 2*; 18–35 yr old, 38 female) participated in the study for monetary compensation ($10 per hour in *experiment 1*, and $15 per hour in *experiment 2*). All participants reported normal or corrected-to-normal vision and provided written, informed consent; the study protocol was approved by the University of Oregon Institutional Review Board (*experiment 1*) and the University of Chicago Institutional Review Board (*experiment 2*).

Participant exclusions for experiment 1. For *experiment 1*, participants were excluded for poor performance on the task and excessive EEG artifacts. One participant did not return for the second day of the experiment. One participant was excluded for poor performance on the first day (86.1° average response error across all *day 1* tests) and data collection was terminated for one participant during the session for excessive artifacts. In addition, participants were excluded from further analysis if they had insufficient artifact-free trials (<550 trials). Artifact number exclusion criteria were set during data collection, but before the data were analyzed. Three participants were excluded due to excessive EEG artifacts. In the final sample, there were 27 participants in *experiment 1* (mean number of artifact-free trials = 799, SD = 85).

Participant exclusions for experiment 2. For *experiment 2*, our target final sample size was 24 subjects. Participants were replaced for poor task performance or if too many trials were lost due to recording or ocular artifacts. One participant was excluded for poor performance on LTM trials (87.1° average response error across all retrieval tests), and data collection was terminated for three participants during the session for excessive artifacts. In addition, participants were excluded from further analysis if they had insufficient artifact-free trials (<450 trials for encoding or retrieval). Artifact number exclusion criteria were set during data collection, but before the data were analyzed. We relaxed the exclusion criterion in *experiment 2* because we obtained fewer trials per condition. Eight participants were excluded due to excessive EEG artifacts. In the final sample there were 24 participants in *experiment 2* (mean number of artifact-free encoding trials = 535, SD = 46 and recall trials = 545, SD = 39).

Apparatus. Stimuli were presented in MATLAB using Psychtoolbox (Brainard 1997; Pelli 1997) and were presented on a 17-in. CRT monitor (60 Hz) for *experiment 1* and on a 24-in. LCD monitor (120 Hz) for *experiment 2*.

Experiment 1 task procedure. The experiment comprised two sessions run on consecutive days (Fig. 1*A*). On *day 1*, participants were instructed to learn 120 object-location associations (see Fig. 1*A* for example clip art) as accurately as possible for the test the next day. On *day 2*, participants were cued with the object and asked to recall and report the associated location while we recorded EEG data.

On *day 1*, all 120 object-location pairings were studied over three repetitions with interleaved retrieval practice. Each of these repetitions were randomly divided into 12 "miniblocks," in which 10 objects were presented followed by a final test on all objects in a random order. Specifically, 10 objects were serially presented in their respective spatial locations (1,000 ms per object, each object initiated by pressing spacebar). Next, each of the 10 objects were presented at fixation in a random order (1,000 ms per object), and participants clicked that object's location along a ring (unspeeded). Recall performance was assessed by calculating the response error (i.e., difference between the presented and reported location, ranging between –180 and 180°). After each response, participants were presented with the object in its correct location and the response error (500 ms). After completing these miniblocks, participants again retrieved all 120 objects in a random order. One participant did not complete the final retrieval on the third run, and one participant accidentally aborted the experiment during the presentation of the first 10 objects before completing the rest of the session.

On *day 2*, participants repeatedly retrieved the location of all 120 objects while we recorded EEG activity (Fig. 1*A*). During each repetition (7–8 in total), the objects were presented in a random order. Each retrieval trial was initiated by a space press. After a variable interval of 1,100 to 1,500 ms, an object was presented at fixation along with the response ring. Participants were instructed to maintain fixation and to avoid blinking or moving the mouse from trial initiation until the cursor appeared 1,250 ms after the onset of the memory cue. Participants were also instructed to recall the location during the retrieval delay (1,250 ms). After each response, participants were shown the correct location of the item along with a number denoting the magnitude of the error.

Experiment 2 task procedure. Experiment 2 was designed to examine encoding-retrieval similarity within a single session. As such, the experiment was modified to take place within 1 day by reducing the total number of objects (80 versus 120). Participants were instructed to learn object-location associations as accurately as possible and that they would alternate between studying and being tested on these associations (Fig. 1*C*).

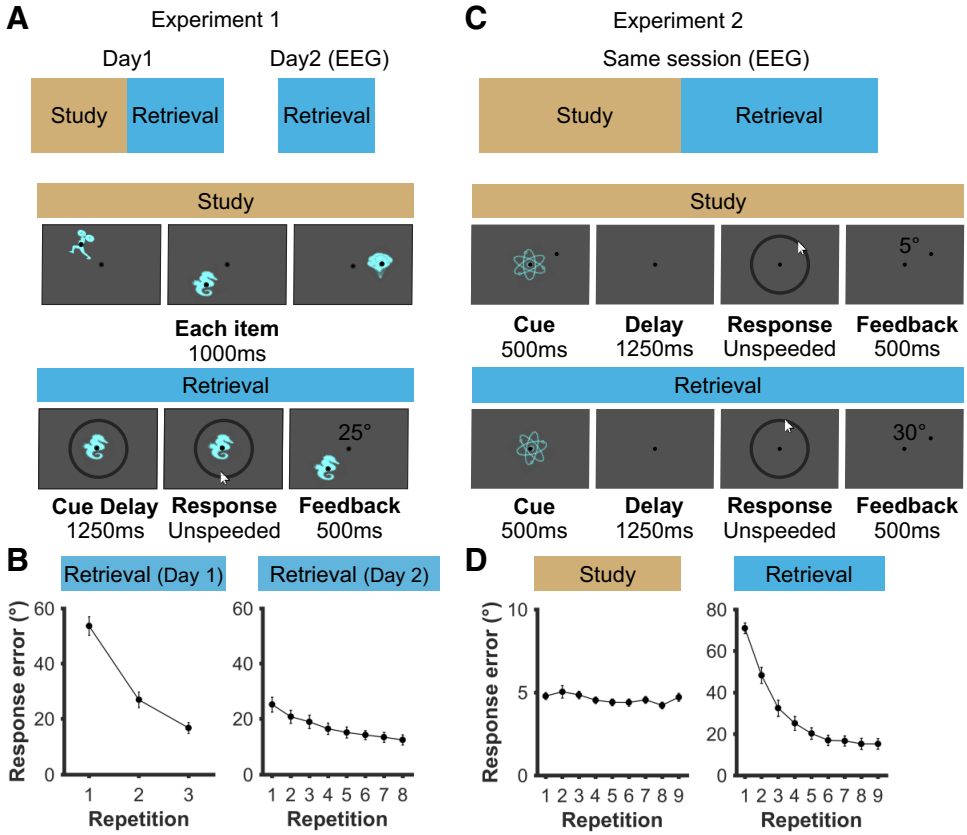

Fig. 1. Task figure and memory performance for *experiments 1* and *2*. *A*: schematic of *experiment 1*, with example study (*experiment 1*, *day 1*) and retrieval (*experiment 1*, *day 2*) trials. Each trial was initiated with a space press. *B*: average absolute error of retrieval responses demonstrating improvements over retrieval repetitions. *C*: schematic of interleaved study and retrieval repetitions in *experiment 2* with example study and retrieval trials. Each trial was initiated with a space press. *D*: average absolute error of study and retrieval responses demonstrating memory accuracy over study and retrieval repetitions. Error bars represent ± 1 SE.

During the study session, participants studied and then recalled each item during each trial. Each study trial was initiated by a space press. After a variable interval of 500 to 800 ms, an object was centrally presented (Fig. 1*C*) along with a dot at the paired location (500-ms stimuli) followed by a blank delay (1,250 ms). To prevent participants from using a part of the object as a reference to remember the associated location, we randomly varied the orientation of each object (−45 to 45°) for each presentation. As in *experiment 1*, participants then reported the to-be-remembered location by clicking on the response ring (unspeeded). Participants were instructed to click with the left mouse button if they were confident in their response, and to click with the right mouse button if they felt that they were guessing. Both confident and guess responses were used for subsequent analyses. After each response, participants were shown the correct location of the item along with a number denoting the magnitude of the error. After studying all 80 objects, participants underwent another retrieval test for all objects in a random order (Fig. 1*C*). The only difference between study and recall trials was the presence of the peripheral dot.

Stimuli. In *experiment 1*, 120 clip art objects (e.g., animals, plants, objects) were selected from the Sutterer and Awh (2016) clip art library. All objects were randomly assigned to unique angular locations (0–360°, 3° steps) for each participant. On *day 1*, the viewing distance was ~80 cm (1.9° stimuli, 5° response ring, 0.3° fixation dot). On *day 2*, the viewing distance was ~100 cm (1.5° stimuli, 4° response ring, 0.25° fixation dot). The background of the screen was medium gray, all objects appeared in the color cyan, the response ring was dark gray, and the fixation dot was rendered in black.

In *experiment 2*, 80 of the objects from *experiment 1* were randomly paired with a unique location drawn from all 360° of possible locations. To assure that the entire space was used, assignment of locations was constrained such that an equal number of locations were drawn without replacement from eight bins each spanning 45° of the possible space. The viewing distance was ~100 cm (1.2° stimuli, 4° response ring, 0.25° fixation dot). The background of the screen was again medium gray, all objects appeared in the color cyan, and the response ring and the fixation dot were dark gray.

Modeling of response errors. Response error was measured as the number of degrees between the presented angular location and the reported angular location. Errors ranged from 0° (a perfect response) to ±180° (a maximally imprecise response). For each run (Fig. 1*B*), we calculated the average absolute response error for the artifact-free trials. Error distributions of this sort have been shown to be well described by a mixture of a uniform distribution for guesses and a Von Mises distribution for correct responses (Brady et al. 2013; Zhang and Luck 2008. We used MemToolbox (Suchow et al. 2013) to calculate the probability of retrieval (P_{mem}), precision (SD), and the bias (μ) of each participants responses.

EEG acquisition. In *experiment 1*, EEG was recorded with 20 tin electrodes mounted in an elastic cap (Electro-Cap International, Eaton, OH). We recorded from International 10/20 sites F3, FZ, F4, T3, C3, CZ, C4, T4, P3, PZ, P4, T5, T6, O1, and O2, along with five nonstandard sites (OL, OR, PO3, PO4, POz). All sites were recorded with a left-mastoid reference and were rereferenced offline to the algebraic average of the left and right mastoids. To detect horizontal eye movements, electrodes were placed ~1 cm from the canthi of each eye to record horizontal electrooculogram (EOG). To detect blinks and vertical eye movements, a single electrode was placed under the center of the right eye and referenced to the left mastoid to record vertical EOG. The EEG and EOG data were amplified with an SA Instrumentation amplifier, filtered (0.01–80 Hz), and digitized (250 Hz) using LabVIEW 6.1 running on a PC.

In *experiment 2*, EEG was recorded from 30 active Ag/AgCl electrodes (Brain Products actiCHamp, Munich, Germany) mounted in an elastic cap positioned according to the International 10–20 system Fp1, Fp2, F7, F3, F4, F8, Fz, FC5, FC6, FC1, FC2, C3, C4, Cz, CP5, CP6, CP1, CP2, P7, P8, P3, P4, Pz, PO7, PO8, PO3, PO4, O1, O2, Oz. A ground electrode was placed in the elastic cap at position FPz. Data were referenced online to the right mastoid and rereferenced offline to the algebraic average of the left and right

mastoids. Incoming data were filtered (0.01–80 Hz) and recorded with a 500-Hz sampling rate using Brain Vision Recorder running on a PC. To detect eye movements and blinks, we used eye tracking to monitor gaze position and EOG activity recorded with five electrodes (~1 cm from the outer canthus of each eye, above/below the right eye, and a ground electrode placed on the left cheek).

Artifact rejection. Data from both experiments were visually inspected for EOG and EEG artifacts. Trials containing blinks, eye movements, blocking, and muscle artifacts were excluded from analysis. One electrode for one participant in *experiment 2* was also rejected during recording because it had malfunctioned. We also monitored gaze position during *experiment 2* using a desk-mounted infrared eye tracking system (EyeLink 1000 Plus, SR Research, Ottawa, ON, Canada). Gaze position data for *experiment 2* were also visually inspected for ocular artifacts. For the analysis of gaze position, we further excluded trials in which the eye tracker was unable to detect the pupil, operationalized as any trial in which the horizontal gaze position was more than 15° from fixation or the vertical gaze position was more than 8.5° from fixation. We collected usable gaze position data (500-Hz sampling rate) for 18 of 24 participants.

Removal of trials with ocular artifacts was effective: maximum variation in grand-averaged horizontal electrooculogram waveforms by remembered location bin was < 2.5 μV for *experiment 1* and < 2 μV for both the encoding and retrieval in *experiment 2*. Thus, eye movements in both experiments corresponded to variations in eye position of $< 0.2°$ of visual angle (Lins et al. 1993), roughly the size of the fixation dot. Analysis of the subset of participants (18) for whom we were able to obtain reliable gaze position data in *experiment 2* corroborates the HEOG data obtained from all participants. Variation in grand-average horizontal gaze position as a function of remembered location was $< 0.11°$ for encoding and $< 0.08°$ of visual angle for retrieval. Variation in grand-average vertical gaze position data by remembered location was $< 0.14°$ for encoding and $< 0.09°$ of visual angle for retrieval. For comparison, HEOG for these participants showed a < 2.1-μV maximum variation which also corresponds to $< 0.2°$ of visual angle.

Time-frequency analysis. To calculate frequency specific activity at each electrode we first band-pass filtered the raw EEG data using EEGLAB (eegfilt, see Delorme and Makeig 2004). Alpha-band analyses were band-pass filtered between 8 and 12 Hz, which is consistent with our prior work (Foster et al. 2016). For our exploratory analysis of the full range of frequencies, we band-pass filtered the data at 1-Hz intervals (4–50 Hz, downsampled to 20 Hz,

$$\text{filter order: } 3 \times \frac{\text{sampling rate}}{\text{low-pass cutoff}}$$

We then applied a Hilbert transform (MATLAB Signal Processing Toolbox) and squared the complex magnitude of the complex analytic signal for each trial to calculate instantaneous power before averaging across trials.

Inverted encoding model. Following our prior work (Foster et al. 2016; Sutterer et al. 2019), we estimated spatially selective channel-tuning functions (CTFs) from the multivariate topographic distribution of oscillatory power across electrodes. We assumed that the power at each electrode reflects the weighted sum of eight spatially selective channels, which we assume reflect the response of neural populations. Each spatially selective channel was tuned for a different angular location (Brouwer and Heeger 2009; Foster et al. 2016; Sprague and Serences 2013; Sprague et al. 2015). We modeled the response profile of each spatial channel across angular locations as a half sinusoid raised to the seventh power:

$$R = \sin(0.5\theta)^7,$$

where θ is angular location (0–359°), and R is the response of the spatial channel in arbitrary units. This response profile was circularly shifted for each channel such that the peak response of each spatial channel was centered over one of the eight location bins which were created relative to the original position of the stimulus. These eight location bins each spanned 45° and were centered on 22.5°, 67.5°, 112.5°, etc. for *experiment 1* and on 0°, 45°, 90°, etc. for *experiment 2*. Bin centers for each experiment were chosen before data collection.

An IEM routine was applied to each time point in the alpha-band analyses and to each time-frequency point in the time-frequency analyses. We partitioned our data into independent sets of training data and test data (for details see *Assignment of trials to training and test sets*). This routine proceeded in two stages (train and test). In the training stage, training data B_1 were used to estimate weights that approximate the relative contribution of the eight spatial channels to the observed response measured at each electrode. Let B_1 (m electrodes $\times$ n_1 observations) be the power at each electrode for each measurement in the training set, C_1 (k channels $\times$ n_1 measurements) be the predicted response of each spatial channel (determined by the basis functions) for each measurement, and W (m electrodes $\times$ k channels) be a weight matrix that characterizes a linear mapping from "channel space" to "electrode space." The relationship between B_1, C_1, and W can be described by a general linear model of the form

$$B_1 = WC_1$$

The weight matrix was obtained via least-squares estimation as follows:

$$\hat{W} = B_1 C_1^T \left(C_1 C_1^T\right)^{-1}$$

In the test stage we inverted the model to transform the observed test data B_2 (m electrodes $\times$ n_2 observations) into estimated channel responses, C_2 (k channels $\times$ n_2 measurements), using the estimated weight matrix, $\hat{W}$, that we obtained in the training phase:

$$\widehat{C_2} = \left(\hat{W}^T\hat{W}\right)^{-1}\hat{W}^T B_2$$

Each estimated channel response function was then circularly shifted to a common center (i.e., 0° on the "Channel offset" axis of Fig. 2*A*) by aligning the estimated channel responses to the channel tuned for the cued/target location to yield the CTF averaged across the eight remembered locations.

Finally, because the exact contributions of each spatial channel to each electrode (i.e., the channel weights, W) varies across participants, we applied the IEM routine separately for each participant, and statistical analyses were performed on the reconstructed CTFs. This approach allowed us to disregard differences in how location-selective activity is mapped to scalp-distributed patterns of power across participants, and instead focus on the profile of activity in the common stimulus or "information" space (Foster et al. 2016; Sprague et al. 2015).

Assignment of trials to training and test sets. Artifact-free trials were partitioned equally into three independent sets to be used as training and test data for the IEM procedure (see *Inverted encoding model*). We downsampled the data so that each set contained an equal number of trials and each location bin within a set also contained the same number of trials. For each of these sets we averaged power across trials for each location bin. We used a cross-validation routine such that two sets of estimated power served as the training data and the remaining set served as the test data. We applied the IEM routine using each of the three matrices as test data, and the remaining two matrices as training data. The resulting CTFs were averaged across each test set.

For the analysis in which we ruled out the possibility that the IEM was detecting object-specific information, we assigned all trials with the same object to the same partition. After completing this additional step, we equated trials across sets and bins in the same manner described above.

For analyses in which we examined how within participant changes in selectivity related to behavior, we first downsampled to equate the

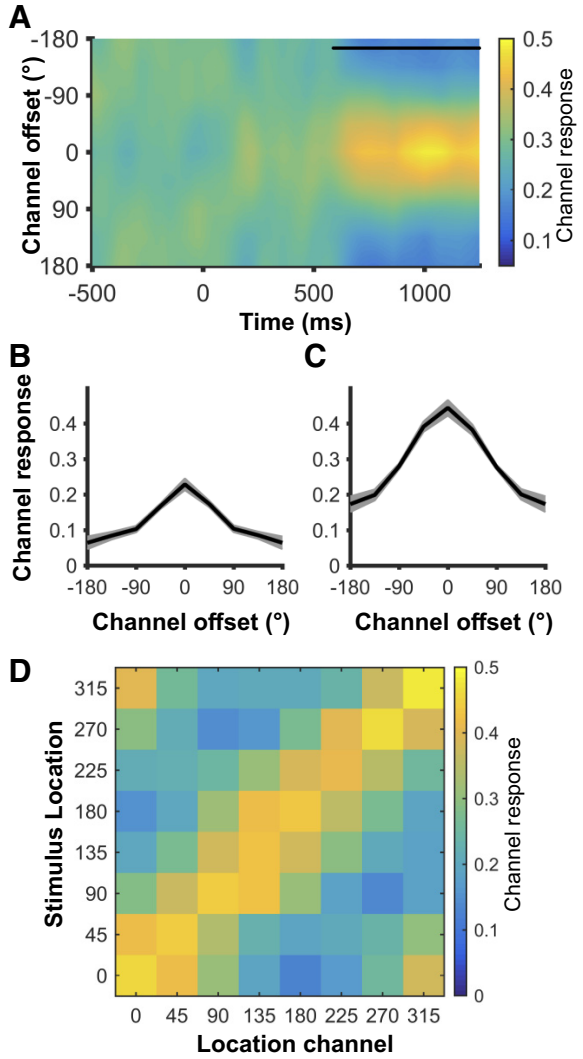

Fig. 2. Alpha-band (8–12 Hz) channel tuning functions (CTFs) from *experiment 1*. *A*: alpha CTF across time. An inverted encoding model was used to reconstruct spatially selective CTFs from the topographic distribution of alpha-band power. CTF selectivity was reliable from 588 to 1,250 ms (quantified as CTF slope; $P < 0.05$, indicated by the black marker). *B*: alpha CTF derived with a set of 8 delta functions and averaged across significant time points (588–1,250 ms). Delta function CTFs are graded confirming that the signal carried by the topography of alpha-band power is intrinsically graded. Thus, the use of a graded basis set is appropriate. Shaded area represents ± 1 SE. *C*: alpha CTF derived with a graded basis set and averaged across significant time points (588–1,250 ms). Shaded area represents ± 1 SE. *D*: channel responses for each of the eight stimulus location bins averaged across significant time points (588–1,250 ms). The channel response peaks at the channels preferred location, indicating that alpha activity is selective for the specific remembered location.

number of trials assigned from each location across conditions. After completing this additional step, we equated trials across sets and bins in the same manner described above. Finally, we employed the same training procedure described above (2/3 of the total data) but split the final test set into our comparisons of interest. Thus, we used the same training data for both conditions and only the test data varied for each comparison.

For analyses that assessed relationships between CTF selectivity and behavior across participants we downsampled the number of trials assigned to each location bin for each of the three sets to be equal to the smallest number of trials assigned to each bin in each set for any participant. This downsampling approach precluded individual differences in CTF selectivity driven by the number of the trials included in the analysis for each participant.

In *experiment 2*, we sought to compare encoding and retrieval-related activity. We closely followed the procedure that examined retrieval-related activity alone, by training on 2/3 of the encoding data and testing on 1/3 of the retrieval data. By maintaining these same ratios of training to test data, we could more directly compare the results from encoding and retrieval.

Resampling random assignment. To avoid spurious results due to the random assignment of trials, we repeated each analysis multiple times with a different random assignment of trials. When comparing between conditions, we conducted 500 iterations per time point. When comparing against a permuted null distribution (which is a time-consuming procedure), we conducted 10 iterations per time point, given the computational time needed for each analysis. To decrease computation time further for the 4–50 Hz time-frequency analysis, we downsampled the data matrix of power values to one sample every 20 ms. We downsampled after calculating power so that downsampling did not affect our calculation of power. The data matrix was not downsampled for analyses restricted to the alpha band.

Calculating CTF selectivity. To quantify selectivity at each time point we calculated the slope of the CTF via linear regression. We collapsed across channels of equidistance (e.g., ± 2 bins). As such, higher slope values indicate greater CTF selectivity while lower values indicate less CTF selectivity.

To test whether CTF selectivity was reliably above chance, we tested whether CTF slope was greater than zero using a one-sample *t*-test. Because mean CTF slope may not be normally distributed under the null hypothesis, we employed a Monte Carlo randomization procedure to empirically approximate the null distribution of the *t*-statistic. To generate our null distribution, we randomly shuffled the remembered location labels in each training/test set so that the labels were random with respect to the observed responses at each electrode. We then repeated 1,000 iterations of this randomization procedure to obtain a null distribution of *t*-statistics at each time point.

Finally, to test whether CTF selectivity was reliably above chance we employed a nonparametric cluster approach that corrects for multiple comparisons by taking into account autocorrelation in time and frequency (Cohen 2014; Maris and Oostenveld 2007). Specifically, we applied a *t*-value threshold corresponding to $P < 0.05$ (*experiment 1*: $t = 1.706$; *experiment 2*: $t = 1.714$) to identify clusters of pixels (time and frequency analysis) or adjacent time points (alpha only analysis). At the same time, we applied the same threshold to each permutation and calculated the largest summed *t*-statistic for any cluster in the permutation, resulting in a distribution of maximal summed *t*-statistics for our permuted null distribution. Finally, the sizes of the significant clusters of the nonpermuted data were thresholded such that only clusters larger than the 95th percentile of the permuted distribution were considered reliable (Type 1 error less than 0.05). Therefore, our cluster test was a one-tailed test, corrected for multiple comparisons.

RESULTS

Experiment 1

Experiment 1 was designed to test whether EEG activity tracked the retrieval of precise spatial locations from LTM. The design includes two important properties. First, we asked subjects to precisely report a remembered location using a continuous report procedure (Wilken and Ma 2004; Zhang and Luck 2008). This provides a sensitive test of memory accuracy as the deviation from the correct location. Second, we recorded EEG activity during memory retrieval for the purposes of building and evaluating an encoding model. This inverted

encoding model (IEM) can track memory retrieval as a graded function of spatial location.

Behavioral performance. On *day 1*, participants studied 120 object-location associations (Fig. 1*A*). On *day 2*, participants returned for a retrieval session in which we recorded EEG. Participants received feedback based on their response error (−180° to 180°). During both days, their performance improved (Fig. 1*B*). During *day 1*, average response error improved significantly from the first [mean (M) = 53.6°, SD = 17.7°] to the final test (M = 17.6°, SD = 11.1°] of the session [$t(26) = 13.2$, $P < 0.001$, two-tailed). As a result on continued feedback, memory also improved from the first (M = 25.2°, SD = 14.1°) to the final test (M = 12.7°, SD = 9.3°) during the second session [$t(26) = 7.3$, $P < 0.001$, two-tailed].

Alpha-band (8–12 Hz) topography tracks spatial representations retrieved from LTM. In *experiment 1*, we tested whether oscillatory EEG activity tracks the time-resolved retrieval of precise spatial memories. Because we have previously found that alpha-band activity tracks spatial locations held in working memory (Foster et al. 2016), we were a priori interested in whether alpha-band power would also track locations retrieved from long-term memory. Thus, we used an IEM to test whether the multivariate topography of alpha-band power tracked locations retrieved from long-term memory. If the pattern of alpha-band power contains spatially selective information about the remembered location, we would expect to see a channel tuning function (CTF) with a peak response in the channel tuned for the remembered location (a channel offset of 0° in Fig. 2) following the retrieval cue. This pattern can be quantified as slope across the position channels as distance from the retrieved location increases. A slope of zero reflects no spatial selectivity in the CTF, while a positive slope reflects spatial selectivity for the location associated with the cue. To test this hypothesis, we conducted a permutation test (see MATERIALS AND METHODS) to determine at which time points we observed a CTF slope that was reliably above zero. We detected reliable selectivity for spatial information (i.e., slopes > 0) that was sustained during the retrieval interval (588–1,250 ms; Fig. 2*A*).

One possibility is that this graded tuning is an artifact of our selection of a graded basis set (Ester et al. 2015; Foster et al. 2016; Saproo and Serences 2014). To investigate this possibility, we reran this analysis using a delta-function basis set that predicts a peak response in the preferred channel and no response in adjacent channels. If the topography of alpha power represents spatial locations in a graded manner, we would still expect a graded pattern of responses. Instead, if the observed results were driven by our selection of a basis set, we would expect a peak response in the correct bin and a little to no response in all other bins. Using a delta function basis set, we observed a graded pattern of responses across remembered locations (Fig. 2*B*) that is similar to the pattern of activity we see when we apply the standard basis set (Fig. 2*C*). This suggests that our results are not an artifact of our selection of a basis set but reflect a real graded tuning profile during the retrieval of spatial memories.

Although the aggregate results revealed that channel activity peaked at the remembered location and dropped in a graded fashion as the distance form that location increased, this analysis did not establish that this orderly pattern was present at each location. Indeed, a coarser hemifield or quadrant-based signal could produce such a pattern. If alpha-band activity precisely tracks retrieved spatial locations, we should observe a graded pattern for each remembered location. We examined the average channel response during time points where we previously observed reliable spatial selectivity (588–1,250 ms) for eight location bins separately (Fig. 2*D*). The channel response for each location revealed graded information throughout the same window, and the channel responses for all locations were significant (All slopes > 0.05, all P values < 0.002). Therefore, alpha-band CTFs track memory retrieval of a precise spatial location.

Identifying frequencies that track the retrieval of spatial location. A motivating question for the present work was whether spatially selective information was specific to alpha-band activity. On the one hand, prior work has found that alpha-band activity selectively tracks spatial locations that are covertly attended (Foster et al. 2017b) or held in working memory (Foster et al. 2016). On the other hand, theta-band (4–7 Hz) and beta-band (16–25 Hz) activity are known to play an important role in long-term memory (Kerren et al. 2018; Morton and Polyn 2017; Nyhus and Curran 2010). Therefore, we performed the same IEM analysis at each frequency and time point from 4 to 50 Hz to test whether other frequency bands also carried spatially selective information about the remembered location. We conducted a permutation test at each frequency and time point and used a cluster correction to identify frequencies with CTFs that were reliably above zero (Fig. 3*A*). The most robust and sustained selectivity was in the alpha band (~400–1,250 ms).

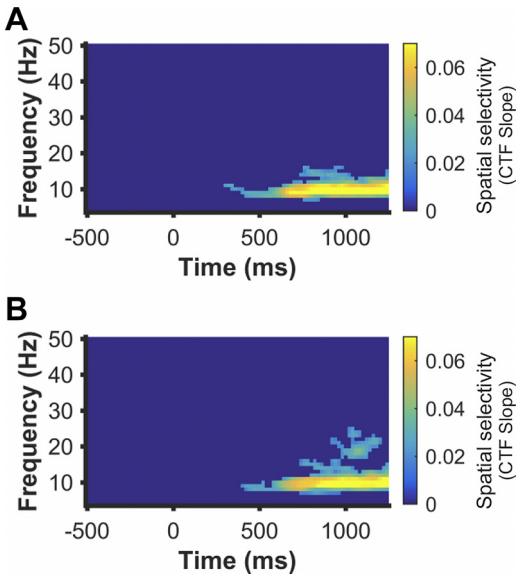

Fig. 3. Identifying frequencies that track retrieved locations for *experiment 1*. *A*: an inverted encoding model (IEM) was used to reconstruct spatially selective channel tuning functions (CTFs) from the topographic distribution of total power across a range of frequencies (4–50 Hz). Alpha power tracked retrieval of spatial information. *B*: training and testing across shapes. Alpha power continued to track the retrieval of spatial information when the IEM was trained and tested on separate shape cues, indicating that CTFs reflect remembered locations not the retrieval cue. Points at which CTF slope values were not reliably above zero as determined by a cluster corrected permutation test ($P < 0.05$) were set to dark blue.

Spatially selective alpha-band activity generalizes across visual objects associated with the same spatial location. For each participant, each object was associated with a unique location such that object and position were confounded within this analysis. Thus, it is possible that the selectivity we observed across some or all frequencies, reflects patterns of activity elicited by the cue rather than activity related to the retrieval of a spatial position. To investigate this, we reran the analysis while ensuring that distinct items were included in the training and test sets (see MATERIALS AND METHODS). Despite this constraint, we observed similar results (Fig. 3*B*), confirming that the sustained spatial selectivity we observed reflected the position associated with each cue rather than the cue itself. Thus, for all subsequent IEM analyses we do not constrain assignment to training and test sets by cue. We also observed a brief period of spatial selectivity in the beta range (16–25 Hz); however, we note that this activity was not observed when we did not constrain the assignment of items to training and test sets.

Spatial selectivity of alpha-band activity increases with repetition and feedback. A consequence of providing feedback during *day 2* is that memory performance improved throughout the session. To examine whether alpha-band CTFs tracked these broad behavioral improvements, we split the test data into the first half and second half of trials. Behaviorally, we observed that memory performance improved from the first half (M = 20.3°, SD = 11.9°) to the second half (M = 13.9°, SD = 9.4°) of the session [$t(26) = 7.2$, $P < 0.001$, two-tailed, Fig. 4*A*]. Furthermore, a mixture model was used to assess whether these decreases in average response error were driven by changes in the probability of retrieval and/or mnemonic precision (see MATERIALS AND METHODS). During *day 2*, the probability of retrieval (P_{mem}) increased over time [first half: M = 86.3%, SD = 13.6%; second half: M = 93.6%, SD = 9.5%; $t(26) = -6.3$, $P < 0.001$, two-tailed] and mnemonic precision improved over time [first half: M = 13.6°, SD = 3.7°; second half: M = 12.3°, SD = 4.1°, $t(26) = 5.52$ $P < 0.001$, two-tailed]. If alpha-band CTFs are sensitive to memory performance, we would expect greater spatial selectivity in the second versus first half of the session. To test this prediction, we isolated the time points where aggregate data revealed significant alpha CTFs (Fig. 2*A*; 588 ms after cue onset until the response) and then compared average CTF slope across the first and second halves of the study. Indeed, spatial selectivity was significantly higher for the second half (CTF slope, M = 0.085, SD = 0.061) relative to the first half (M = 0.06, SD = 0.055) of the experiment [$t(26) = -3.29$, $P = 0.003$, two-tailed; Fig. 4*B*].

This reveals that alpha-band activity tracks the improvement in memory performance across learning episodes. Finally, CTF selectivity across the same window did not predict between-subject variations in the accuracy of recall [$\rho(26) = -0.11$, $P = 0.6$]. This null result could have numerous explanations but here we offer one hypothesis. While we instructed participants to immediately recall the location that corresponded to the object cue, it may be that some participants waited longer than others to call the correct location to mind while other participants relied on a more prospective strategy in which they immediately recalled the target location. This kind of strategic difference could yield large differences in mean CTF slope that may have been unrelated to whether the critical item could be retrieved. Indeed, the response time analysis in the next section lends further plausibility to this hypothesis.

Spatially selective alpha-band activity tracks within- and between-subject variations in response latency. The latency of memory retrieval varied across trials and participants to a large extent (see Fig. 5*A*). To examine whether alpha-band CTFs tracked these behavioral differences in response time (RT), we split the test data into two halves based on the median RT (average fast RT: M = 854 ms, SD = 241 ms; average slow RT: M = 1,961 ms, SD = 1,055 ms). If alpha-band CTFs track the latency of memory retrieval, we would expect greater location selectivity on trials in which participants responded more quickly. Indeed, location selectivity was significantly greater when participants responded more quickly (M = 0.085, SD = 0.054) than when they responded slowly [M = 0.051, SD = 0.060; $t(26) = -4.29$, $P < 0.001$, two-tailed; Fig. 5*B*]. This pattern supports the hypothesis that participants responded more quickly when they had already retrieved the spatial information before the onset of the response cue, yielding a higher level of CTF selectivity during trials with faster responses.

Across participants, we observed substantial variation in median RTs (range = 504–2,025 ms). To examine whether alpha-band CTFs tracked these individual differences in behavior, we tested whether there was a correlation between median RT and the selectivity of alpha-band CTFs (measured as slope). We predicted that participants who responded more quickly (i.e., faster RTs) would also have greater spatial selectivity (i.e., higher CTF slope). We observed a trending negative relationship between RT and CTF slope, as predicted ($\rho = -0.36$; $P = 0.07$; Fig. 5*C*). In addition to reflecting differences in the immediate accessibility of spatial memories, this relationship could also be driven by individual differences in the extent to which participants engaged in prospective retrieval during the delay interval. This is our working hypoth-

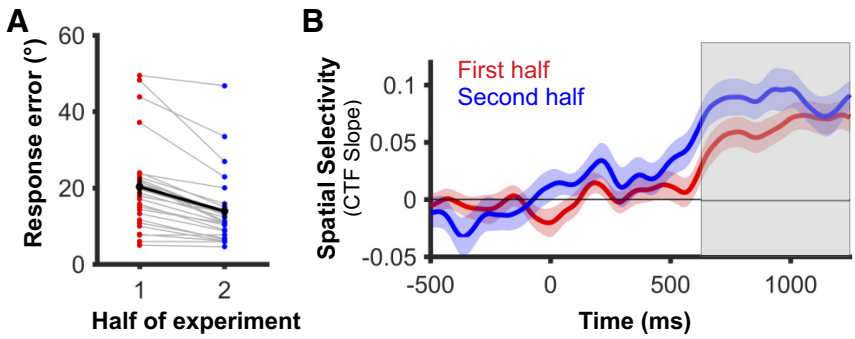

Fig. 4. Assessing the relationship between alpha selectivity and memory performance for experiment 1. *A*: average response error improved from the first to the second half of the experiment ($P < 0.001$). Error bars represent ± 1 SE. *B*: time-resolved channel tuning function (CTF) slopes for trials from the first and second half of the experiment. CTF slope reflects learning across the session and reveals significantly higher spatial selectivity for the second half of the experiment relative to the first half ($P = 0.003$). Reliable differences were assessed by averaging across time points where we observed reliable CTFs for all trials (gray box) and comparing CTF slope between the first and second half of the experiment. Shaded error bars represent ± 1 SE.

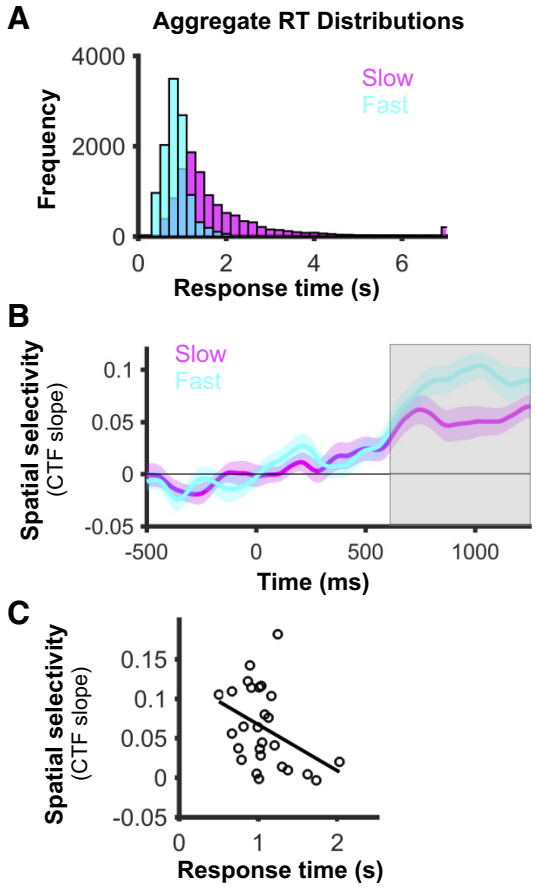

Fig. 5. Assessing the relationship between alpha selectivity and response times (RT) for *experiment 1*. *A*: aggregate distribution of all participants' fast and slow response times. Response times > 7 s are represented in the last bin of the histogram. *B*: time-resolved channel tuning function (CTF) slope for trials with the fastest and slowest response times. CTF slope reflects response latency and reveals that spatial selectivity was higher for trials when participants responded quickly ($P < 0.001$). Reliable differences were assessed by averaging CTF slope across time points where we observed reliable CTFs for all trials (gray box) and comparing CTF slopes for slow and fast trials. Shaded error bars represent ± 1 SE. *C*: alpha selectivity is modestly correlated with response times across subjects although the relationship is not significant [$\rho(26) = -0.36$ $P = 0.07$].

esis, given that the differences in response latency seemed too large to reflect differences in the immediate accessibility of the spatial memories alone.

Experiment 2

In *experiment 2*, we replicated and extended *experiment 1* in two important ways. First, to further examine the relationship between alpha-band selectivity and memory performance, we recorded EEG data throughout the learning process, including the first retrieval attempts. Second, we recorded EEG during both encoding and retrieval, which allowed us to test the extent that retrieval-related oscillatory activity resembled encoding-related oscillatory activity.

Behavioral performance. During a single session, participants learned 80 object-location associations (Fig. 1*C*) with interleaved study and retrieval. During study trials, participants actively maintained the associated spatial location over a 1,250 ms delay interval. During retrieval trials, participants had to retrieve the associated spatial location from long-term memory. During study trials, memory performance was very accurate and improved modestly but reliably from the first half (M = 4.7°, SD = 1°) to the second half (M = 4.4°, SD = 0.9°) of the session [$t(23) = 2.42$, $P = 0.024$, two-tailed; Fig. 1*D*]. Mixture modeling revealed that this change was due to an improvement in mnemonic precision [first half: M = 5.8°, SD = 1.2°; second half: M = 5.4°, SD = 1.1°; $t(23) = 2.28$, $P = 0.032$ two-tailed] while no change was observed for probability of retrieval [first half: M = 99.9%, SD = 0.30%; second half: M = 99.9%, SD = 0.16%; $t(23) = -0.82$, $P = 0.42$, two-tailed], which was at ceiling. For the LTM retrieval trials, we observed a substantial improvement in memory performance across the session as learning progressed. Memory error decreased from the first half (M = 40.8°, SD = 14.0°) to the second half [M = 16.2°, SD = 11.9°; $t(23) = 17.0$, $P < 0.001$, two-tailed; Fig. 6*A*] of the experiment. We replicated our finding from *experiment 1* that the reduction in memory error was driven by both an increase in the probability of retrieval [first half: M = 61.1%, SD = 16.1%; second half: M = 89.9%, SD = 13.9%; $t(23) = -15.4$, $P < 0.001$, two-tailed] and an improvement in mnemonic precision [first half: M = 13.7°, SD = 4.4°; second half: M = 11.3°, SD = 2.7°; $t(23) = 4.12$, $P < 0.001$, two-tailed]. Thus, long-term memory improved throughout the session as participants learned the object-location associations.

One goal for *experiment 2* was to create a larger range of performance throughout the session in which EEG data were recorded. In line with this goal, we observed a much larger range in mean response error in *experiment 2* (71.0° *run 1*–15.2° *run 9*; Fig. 1*D*) than in *day 2* of *experiment 1* (25.2° *run 1*–12.3° *run 8*), giving us the opportunity to apply the IEMs approach across the full trajectory of learning.

Spatial selectivity of alpha-band activity increases with repetition and feedback. In *experiment 1*, alpha-band CTFs tracked retrieval of spatial locations from long-term memory. Furthermore, spatial selectivity of alpha-band CTFs increased as memory performance improved with repetition and feedback (Fig. 4). *Experiment 2* was designed to replicate and extend those results over a larger range of behavior. We predicted that alpha-band CTFs would demonstrate higher selectivity when memories were more accurate. In line with this prediction, the average selectivity (i.e., CTF slopes) was larger in the second half of the session (M = 0.048, SD = 0.033) than in the first half [M = 0.012, SD = 0.022; $t(23) = -4.79$, $P < 0.001$; two-tailed; Fig. 6*B*]. Note, for this and all subsequent average CTF analyses, we averaged from 588 ms (the starting time point used in *experiment 1*) until the onset of the response cue. Control analyses revealed that increases in alpha-selectivity across the session could not be attributed to increases in alpha power across the recoding session (Supplemental Fig. S1; https://figshare.com/s/9f594406315b89b21e9a). As in *experiment 1*, CTF slope did not track memory performance between participants [$\rho(23) = -0.14$, $P = 0.52$]. Thus, the spatial selectivity of alpha activity tracked broad improvements in memory performance across the session, but not individual differences in memory performance.

Spatially selective alpha-band activity tracks response latency. As in *experiment 1*, we found that the selectivity of alpha-band CTFs tracked within- and between-subject variations in RT (Fig. 7). A median split on RT revealed greater spatial selectivity for trials with fast RTs (CTF slope: M =

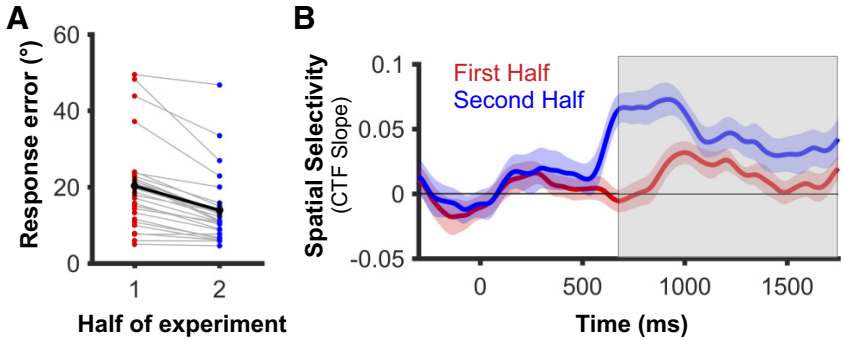

Fig. 6. Assessing the relationship between alpha selectivity and memory performance for *experiment 2*. *A*: average response error improved from the first to the second half of the experiment ($P < 0.001$). Error bars represent ± 1 SE. *B*: time-resolved channel tuning function (CTF) slopes for trials from the first and second half of the experiment. CTF slope reflects learning across the session and reveals significantly higher spatial selectivity for the second half of the experiment relative to the first half ($P < 0.001$). Reliable differences were assessed by averaging across time points where we observed reliable CTFs for all trials (gray box) and comparing CTF slope between the first and second half of the experiment. Shaded error bars represent ± 1 SE.

0.035, SD = 0.03) than trials with slow RTs [M = 0.021, SD = 0.018, $t(23) = -2.53$, $P = 0.019$, two-tailed; Fig. 7*B*). We also replicated our finding that participants with faster RTs showed greater spatial selectivity of alpha-band CTFs ($\rho = -0.49$; $P = 0.02$; Fig. 7*C*). This link between CTF slope and RTs may reflect strategic differences between participants who prospectively recalled the associated location quickly following cue onset and those that waited until closer to the response window to bring that information to mind.

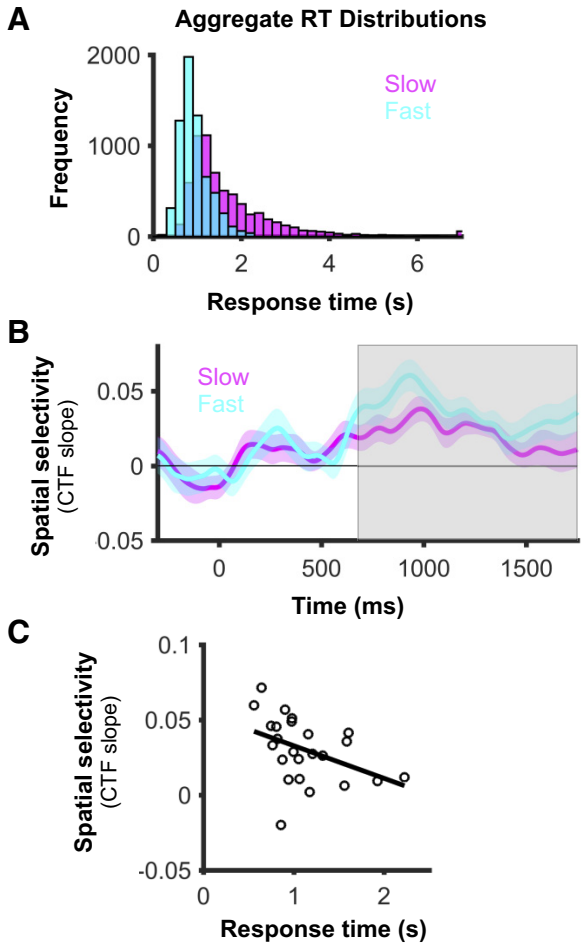

Fig. 7. Assessing the relationship between alpha selectivity and response times (RT) for *experiment 2*. *A*: aggregate distribution of all participants' fast and slow response times. Response times > 7 s are represented in the last bin of the histogram. *B*: time-resolved channel tuning function (CTF) slope for trials with the fastest and slowest response times. CTF slope reflects response latency and reveals that spatial selectivity was higher for trials when participants responded quickly ($P = 0.019$). Reliable differences were assessed by averaging CTF slope across time points where we observed reliable CTFs (gray box) for all trials and comparing fast and slow trials. Shaded error bars represent ± 1 SE. *C*: alpha selectivity is modestly correlated with response times across subjects [$\rho(23) = -0.49$ $P = 0.02$].

Comparing frequency specificity at encoding and retrieval. In *experiment 1*, we found that oscillatory activity in the alpha band (8–12 Hz) tracked retrieved locations following a memory cue. In *experiment 2*, we replicated this finding, with cluster corrected permutation tests showing that primarily oscillations between 8 and 12 Hz (~500–1,500 ms; Fig. 8*A*), and to a lesser extent, oscillations between 12 and 20 Hz (~900–1200 ms; Fig. 8*A*), tracked the retrieved location. Note that, to obtain the most robust measurement of spatially sensitive frequencies at retrieval, we only tested our IEM on trials from the second half of the experiment when memory performance and spatial selectivity were highest (Fig. 6, *A* and *B*). For consistency, we applied the same approach to study trials. Applying the IEM to study trials revealed that spatially selective information was represented across a wider range of low frequencies (Fig. 8*B*; 4–8 Hz, 0–500 ms; 8–20 Hz, ~200–1,750 ms; 20–30 Hz, ~1,500–1,750 ms) than during retrieval. However, we observed the most sustained spatial selectivity across the delay period in the alpha band (8–12 Hz). These results replicate past work showing that alpha-band activity tracks locations held in working memory (Foster et al. 2016; Sutterer et al. 2019). Finally, an overlay plot of frequency bands carrying spatially specific information in both the encoding and retrieval tasks (Fig. 8*C*) revealed considerable overlap in the 8–12 Hz band across conditions. Together these findings reveal that there is substantial, although not complete, overlap in the range of frequencies carrying spatially specific information during memory encoding and retrieval.

Patterns of alpha-band activity generalize across encoding and retrieval. While the same frequency band carried spatial information during both study and retrieval, this does not necessarily mean that the multivariate patterns of activity corresponding to each location are also similar during encoding and retrieval. To provide a comprehensive test of encoding-retrieval similarity, we trained the IEM using study trials and tested the model on retrieval trials. We observed robust spatial selectivity throughout the retrieval interval (520–1,750 ms; $P < 0.05$; Fig. 9). This provides evidence that the multivariate pattern of alpha activity during retrieval is well described as a reinstantiation of the pattern of alpha-band activity seen during encoding.

DISCUSSION

The present work represents a new approach for tracking and understanding the neural mechanisms underlying retrieval of

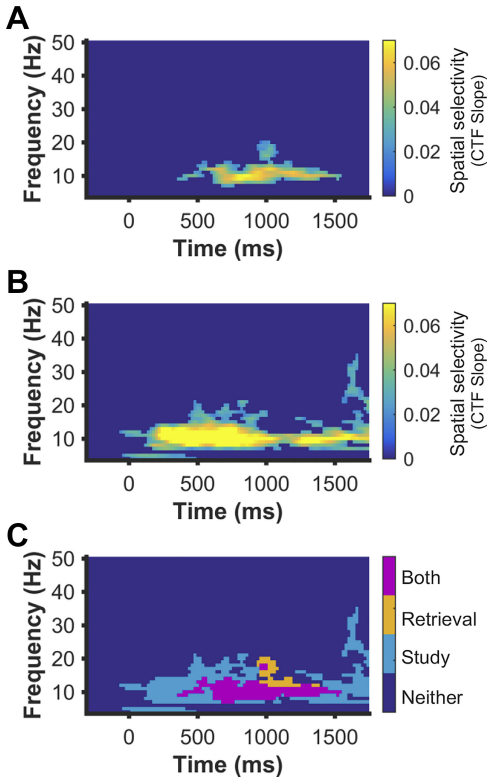

Fig. 8. Identifying frequencies that track encoded and retrieved locations for *experiment 2*. An inverted encoding model was used to reconstruct spatially selective channel tuning functions (CTFs) from the topographic distribution of total power across a range of frequencies (4–50 Hz) at retrieval and study. To ensure robust retrieval memory performance, only trials from the second half of the session were used in the test set for this analysis. *A*: primarily alpha power tracked spatial information during retrieval trials. *B*: initially and at the end of the delay, a broad range of frequencies tracked the encoded location (4–35 Hz) while primarily alpha power tracked the remembered location through the entire delay. *C*: overlay plot of significant activity during retrieval and study. Teal points reflect reliable spatial selectivity during study, orange points reflect reliable selectivity at retrieval, and magenta points reflect overlap selectivity at study and retrieval. Points at which CTF slope values were not reliably above zero as determined by a cluster corrected permutation test ($P < 0.05$) were set to dark blue.

precise feature memories. In two experiments, we employed a combination of a continuous report task, in which participants learned to associate individual objects with specific spatial locations, with the application of an inverted encoding model (IEM) to ongoing EEG activity. Using an IEM, we showed that rhythmic brain activity enables temporally resolved tracking of the retrieval of precise spatial locations from long-term memory.

A novel aspect of our work was the ability to search for frequencies that code for precise spatial memories. Recent theories about the role of neural oscillations in memory propose that both the frequencies supporting cognitive operations at encoding and retrieval and the specific patterns of activity within those frequencies should overlap (Siegel et al. 2012; Watrous and Ekstrom 2014; Watrous et al. 2015). In line with this prediction, we observed considerable overlap in the frequencies carrying spatial memory representations between encoding and retrieval. Specifically, we observed sustained spatial selectivity, primarily in the alpha band (8–12 Hz), during both study and long-term memory retrieval. We also found that the multivariate patterns of alpha-band activity reinstated during retrieval are similar to those patterns observed during the initial encoding of locations. These observations provide new evidence that encoding-retrieval oscillatory similarity extends to the representation of precise feature representations at the population level, supporting the idea that oscillatory brain activity plays a critical role in memory formation and reinstatement. However, it is worth noting that a broader range of frequencies tracked to-be-remembered locations at study than at retrieval, suggesting that not all spatially sensitive frequencies engaged during stimulus presentation are later reinstated.

The observation that alpha-band activity tracks retrieved spatial memories is similar to what has been observed during visual working memory maintenance (Foster et al. 2016, 2017a; Sutterer et al. 2019) and is consistent with work that suggests a role for alpha in memory retrieval and memory-guided attention (Fukuda and Woodman 2017; Stokes et al. 2012; Waldhauser et al. 2016). However, this stands in contrast with other findings that suggest an important role of theta and beta activity in long-term memory. We observed relatively little spatial selectivity in the beta-band during memory retrieval, which is consistent with the notion that beta-band (15–25 Hz) activity may be more important for the encoding and retrieval of category-specific information (Morton and Polyn 2017; Morton et al. 2013) rather than spatial information. While past studies have found that theta-band activity (4–7 Hz) plays a key role in episodic memory (Hsieh and Ranganath 2014; Kerren et al. 2018; Nyhus and Curran 2010) and in the hippocampus during spatial navigation (Bohbot et al. 2017; Watrous et al. 2011), it is likely that our scalp EEG signal is insensitive to theta signals prominent in the hippocampus (Hsieh and Ranganath 2014). Future work from modalities that more directly index hippocampal activity (i.e., intracranial recordings from the hippocampus) or use source reconstruction to isolate activity originating in the medial temporal lobe (Kerren et al. 2018) might provide insight into the role of theta activity in precise spatial memory reinstatement.

Another promising application of the approach employed here is the ability to compare the time course with which fine-grained and coarser memory representations emerge. For example, spatially selective alpha activity emerged considerably later than some prior observations of hemifield-selective activity. While hemifield selective activity has been observed within 200 ms of the onset of a retrieval cue (Waldhauser et al. 2016), our time by frequency analysis revealed no evidence of activity related to the specific retrieved location, in any fre-

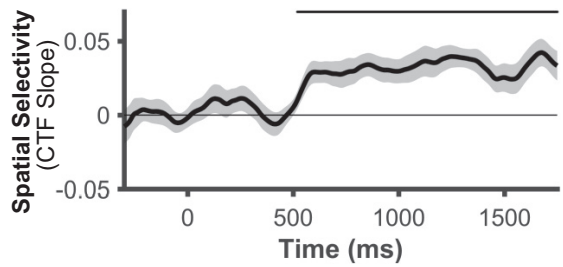

Fig. 9. Testing whether the multivariate patterns of alpha power at study are reinstated at retrieval. Alpha power tracks the retrieval of spatial information when the inverted encoding model was trained on study data and tested on retrieval data, indicating that the pattern of alpha-band activity observed during study is reactivated at retrieval. Shaded error bars represent ± 1 SE. Markers on the top of the plot mark the periods of reliable spatial selectivity ($P < 0.05$). CTF, channel tuning function.

quency band, until ~400 ms after the retrieval cue. One possible explanation for this latency difference is that hemisphere reactivation and retrieval of fine-grained spatial representations rely on different processes. For instance, Gratton and colleagues (1997) suggest that the hemisphere bias they observed may be more structural, resulting from the formation of a stronger trace in the hemisphere contralateral to the hemifield in which the stimulus was presented. In the present study, the relatively slower onset of alpha CTFs implies a more effortful retrieval of precise spatial information. Another potential explanation is that context reinstatement during an object recognition task could occur more rapidly than object-cued retrieval of spatially selective information. Further work is needed to explore this difference in latency between hemifield effects and the reactivation of the fine-grained alpha topography that tracks specific locations.

We modeled LTM retrieval performance using a mixture modeling approach. This approach is commonplace in the field of visual working memory (Wilken and Ma 2004; Zhang and Luck 2008). More recently, this approach proven useful in the study of LTM (Brady et al. 2013; Harlow and Donaldson 2013; Murray et al. 2015; Richter et al. 2016). A key advantage of the mixture modeling approach is that it provides distinct measures of mnemonic precision and the probability that memories are retrieved (Fan and Turk-Browne 2013; Harlow and Yonelinas 2016; Sutterer and Awh 2016). Initial studies have found that these parameters are reflected by distinct neural signals (Murray et al. 2015; Richter et al. 2016), providing further evidence that separately modeling mnemonic precision and probability of retrieval is a meaningful distinction. Our results demonstrate that both the probability of retrieving long-term memories and the precision with which those memories are retrieved continue to improve with feedback over many repetitions. We propose that this more sensitive approach of assessing memory accuracy will shed new light on long-standing questions in the field.

Does alpha-band activity reflect memory reinstatement?

There is a considerable body of work demonstrating links between alpha-band activity and spatial attention (Foster and Awh 2019; Foster et al. 2017b; Worden et al. 2000). Thus, it is possible that the spatial alpha-band representations we report here reflect sustained attention to studied and remembered locations. This raises the question of whether deployment of covert attention to a remembered location at retrieval qualifies as memory reinstatement. In our view, it does. Reinstatement is typically defined by consistent patterns of activity between encoding and retrieval (Danker and Anderson 2010), and in the present study we observed that both the frequencies and patterns of activity engaged during initial encoding are reengaged during retrieval. We also note that it is well known that it is possible to attend to features and categories. Thus, most demonstrations of category or feature level reinstatement share a similar relationship with attention. In line with this idea, retro-cuing studies have demonstrated that categories (LaRocque et al. 2013; Lewis-Peacock et al. 2012; Rose et al. 2016) or features (LaRocque et al. 2017) that must be attended to prepare for an upcoming test are uniquely decodable, while the features of items that are not necessary for the current probe cannot be decoded. Thus, past and present findings are consistent with the view that there is considerable overlap between attention and memory (Gazzaley and Nobre 2012).

This tight coupling of memory and attention has inspired an active body of research exploring the extent that attention to a stimulus and attention guided by memory are supported by the same neural underpinnings (Summerfield et al. 2006). New fMRI evidence suggests that the networks supporting attention in these cases are not completely overlapping. For instance, hemispheric asymmetries observed in parietal cortex when observers attend a stimulus are not observed when memory guides attention to a stimulus (Rosen et al. 2015), and memory-guided attention engages a different constellation of cortical regions than stimulus guided attention (Rosen et al. 2018). The present work demonstrates that while differences exist in the brain networks that support stimulus and memory-guided attention a similar constellation of oscillatory activity supports both processes.

Conclusion

Prominent models have argued that spatial-temporal context is the backbone of episodic memory (Ekstrom and Ranganath 2018; O'Keefe and Nadel 1978) serving as an index for the retrieval of specific past experiences. Thus, a method that allows temporally resolved tracking of spatial retrieval from LTM may provide a powerful tool for understanding human memory. Here, we present such a method and show that it tracks both the accuracy and latency of memory-guided behavior. Moreover, we provide new evidence confirming a clear prediction of reinstatement models of LTM retrieval. The format of oscillatory activity during encoding into LTM is recapitulated during the subsequent retrieval of those memories.

ACKNOWLEDGMENTS

The authors thank Brendan Colson, Nicholas Diaz, Jared Evans, Ariana Gale, Anubuv Gupta, Dylan Seitz, and William Ngiam for assistance with data collection and Megan deBettencourt for helpful comments on the manuscript.

GRANTS

This work was supported by National Institute of Mental Health Grant R01MH-08721406A1 to E. Awh and E. K. Vogel.

DISCLOSURES

No conflicts of interest, financial or otherwise, are declared by the authors.

AUTHOR CONTRIBUTIONS

D.W.S. and E.A. conceived and designed research; D.W.S. performed experiments; D.W.S. and J.J.F. analyzed data; D.W.S., J.J.F., J.T.S., E.K.V., and E.A. interpreted results of experiments; D.W.S. prepared figures; D.W.S. drafted manuscript; D.W.S., J.J.F., J.T.S., E.K.V., and E.A. edited and revised manuscript; D.W.S., J.J.F., J.T.S., E.K.V., and E.A. approved final version of manuscript.

REFERENCES

Bohbot VD, Copara MS, Gotman J, Ekstrom AD. Low-frequency theta oscillations in the human hippocampus during real-world and virtual navigation. *Nat Commun* 8: 14415, 2017. doi:10.1038/ncomms14415.

Bosch SE, Jehee JFM, Fernández G, Doeller CF. Reinstatement of associative memories in early visual cortex is signaled by the hippocampus. *J Neurosci* 34: 7493–7500, 2014. doi:10.1523/JNEUROSCI.0805-14.2014.

Brady TF, Konkle T, Gill J, Oliva A, Alvarez GA. Visual long-term memory has the same limit on fidelity as visual working memory. *Psychol Sci* 24: 981–990, 2013. doi:10.1177/0956797612465439.

Brainard DH. The Psychophysics Toolbox. *Spat Vis* 10: 433–436, 1997. doi:10.1163/156856897X00357.

Brouwer GJ, Heeger DJ. Decoding and reconstructing color from responses in human visual cortex. *J Neurosci* 29: 13992–14003, 2009. doi:10.1523/JNEUROSCI.3577-09.2009.

Cohen MX. *Analyzing Neural Time Series Data: Theory and Practice*. Cambridge, MA: MIT Press, 2014.

Danker JF, Anderson JR. The ghosts of brain states past: remembering reactivates the brain regions engaged during encoding. *Psychol Bull* 136: 87–102, 2010. doi:10.1037/a0017937.

Delorme A, Makeig S. EEGLAB: an open source toolbox for analysis of single-trial EEG dynamics including independent component analysis. *J Neurosci Methods* 134: 9–21, 2004. doi:10.1016/j.jneumeth.2003.10.009.

Ekstrom AD, Ranganath C. Space, time, and episodic memory: the hippocampus is all over the cognitive map. *Hippocampus* 28: 680–687, 2018. doi:10.1002/hipo.22750.

Ester EFF, Sprague TCC, Serences JTT. Parietal and frontal cortex encode stimulus-specific mnemonic representations during visual working memory. *Neuron* 87: 893–905, 2015. doi:10.1016/j.neuron.2015.07.013.

Fan JE, Turk-Browne NB. Internal attention to features in visual short-term memory guides object learning. *Cognition* 129: 292–308, 2013. doi:10.1016/j.cognition.2013.06.007.

Favila SE, Samide R, Sweigart SC, Kuhl BA. Parietal representations of stimulus features are amplified during memory retrieval and flexibly aligned with top-down goals. *J Neurosci* 38: 7809–7821, 2018. doi:10.1523/JNEUROSCI.0564-18.2018.

Foster JJ, Awh E. The role of alpha oscillations in spatial attention: limited evidence for a suppression account. *Curr Opin Psychol* 29: 34–40, 2019. doi:10.1016/j.copsyc.2018.11.001.

Foster JJ, Bsales EM, Jaffe RJ, Awh E. Alpha-band activity reveals spontaneous representations of spatial position in visual working memory. *Curr Biol* 27: 3216–3223.e6, 2017a. doi:10.1016/j.cub.2017.09.031.

Foster JJ, Sutterer DW, Serences JT, Vogel EK, Awh E. The topography of alpha-band activity tracks the content of spatial working memory. *J Neurophysiol* 115: 168–177, 2016. doi:10.1152/jn.00860.2015.

Foster JJ, Sutterer DW, Serences JT, Vogel EK, Awh E. Alpha-band oscillations enable spatially and temporally resolved tracking of covert spatial attention. *Psychol Sci* 28: 929–941, 2017b. doi:10.1177/0956797617699167.

Fukuda K, Woodman GF. Visual working memory buffers information retrieved from visual long-term memory. *Proc Natl Acad Sci USA* 114: 5306–5311, 2017. doi:10.1073/pnas.1617874114.

Gazzaley A, Nobre AC. Top-down modulation: bridging selective attention and working memory. *Trends Cogn Sci* 16: 129–135, 2012. doi:10.1016/j.tics.2011.11.014.

Gratton G, Corballis PM, Jain S. Hemispheric organization of visual memories. *J Cogn Neurosci* 9: 92–104, 1997. doi:10.1162/jocn.1997.9.1.92.

Harlow IM, Donaldson DI. Source accuracy data reveal the thresholded nature of human episodic memory. *Psychon Bull Rev* 20: 318–325, 2013. doi:10.3758/s13423-012-0340-9.

Harlow IM, Yonelinas AP. Distinguishing between the success and precision of recollection. *Memory* 24: 114–127, 2016. doi:10.1080/09658211.2014.988162.

Hindy NC, Ng FY, Turk-Browne NB. Linking pattern completion in the hippocampus to predictive coding in visual cortex. *Nat Neurosci* 19: 665–667, 2016. doi:10.1038/nn.4284.

Hsieh L-T, Ranganath C. Frontal midline theta oscillations during working memory maintenance and episodic encoding and retrieval. *Neuroimage* 85: 721–729, 2014. doi:10.1016/j.neuroimage.2013.08.003.

Jafarpour A, Fuentemilla L, Horner AJ, Penny W, Duzel E. Replay of very early encoding representations during recollection. *J Neurosci* 34: 242–248, 2014. doi:10.1523/JNEUROSCI.1865-13.2014.

Johnson JD, Price MH, Leiker EK. Episodic retrieval involves early and sustained effects of reactivating information from encoding. *Neuroimage* 106: 300–310, 2015. doi:10.1016/j.neuroimage.2014.11.013.

Kerren C, Linde-Domingo J, Hanslmayr S, Wimber M. An optimal oscillatory phase for pattern reactivation during memory retrieval. *SSRN Electron J*: 1–10, 2018. doi:10.1016/j.cub.2018.08.065

LaRocque JJ, Lewis-Peacock JA, Drysdale AT, Oberauer K, Postle BR. Decoding attended information in short-term memory: an EEG study. *J Cogn Neurosci* 25: 127–142, 2013. doi:10.1162/jocn_a_00305.

LaRocque JJ, Riggall AC, Emrich SM, Postle BR. Within-category decoding of information in different attentional states in short-term memory. *Cereb Cortex* 27: 4881–4890, 2017. doi:10.1093/cercor/bhw283.

Lewis-Peacock JA, Drysdale AT, Oberauer K, Postle BR. Neural evidence for a distinction between short-term memory and the focus of attention. *J Cogn Neurosci* 24: 61–79, 2012. doi:10.1162/jocn_a_00140.

Lins OG, Picton TW, Berg P, Scherg M. Ocular artifacts in recording EEGs and event-related potentials. II: Source dipoles and source components. *Brain Topogr* 6: 65–78, 1993. doi:10.1007/BF01234128.

Maris E, Oostenveld R. Nonparametric statistical testing of EEG- and MEG-data. *J Neurosci Methods* 164: 177–190, 2007. doi:10.1016/j.jneumeth.2007.03.024.

Morton NW, Kahana MJ, Rosenberg EA, Baltuch GH, Litt B, Sharan AD, Sperling MR, Polyn SM. Category-specific neural oscillations predict recall organization during memory search. *Cereb Cortex* 23: 2407–2422, 2013. doi:10.1093/cercor/bhs229.

Morton NW, Polyn SM. Beta-band activity represents the recent past during episodic encoding. *Neuroimage* 147: 692–702, 2017. doi:10.1016/j.neuroimage.2016.12.049.

Murray JG, Howie CA, Donaldson DI. The neural mechanism underlying recollection is sensitive to the quality of episodic memory: event related potentials reveal a some-or-none threshold. *Neuroimage* 120: 298–308, 2015. doi:10.1016/j.neuroimage.2015.06.069.

Nyhus E, Curran T. Functional role of gamma and theta oscillations in episodic memory. *Neurosci Biobehav Rev* 34: 1023–1035, 2010. doi:10.1016/j.neubiorev.2009.12.014.

O'Keefe J, Nadel L. *The Hippocampus as a Cognitive Map*. Oxford, UK: Clarendon, 1978.

Pelli DG. The VideoToolbox software for visual psychophysics: transforming numbers into movies. *Spat Vis* 10: 437–442, 1997. doi:10.1163/156856897X00366.

Polyn SM, Natu VS, Cohen JD, Norman KA. Category-specific cortical activity precedes retrieval during memory search. *Science* 310: 1963–1966, 2005. doi:10.1126/science.1117645.

Richter FR, Cooper RA, Bays PM, Simons JS. Distinct neural mechanisms underlie the success, precision, and vividness of episodic memory. *eLife* 5: e18260, 2016. doi:10.7554/eLife.18260.

Ritchey M, Wing EA, LaBar KS, Cabeza R. Neural similarity between encoding and retrieval is related to memory via hippocampal interactions. *Cereb Cortex* 23: 2818–2828, 2013. doi:10.1093/cercor/bhs258.

Rose NS, LaRocque JJ, Riggall AC, Gosseries O, Starrett MJ, Meyering EE, Postle BR. Reactivation of latent working memories with transcranial magnetic stimulation. *Science* 354: 1136–1139, 2016. doi:10.1126/science.aah7011.

Rosen ML, Stern CE, Devaney KJ, Somers DC. Cortical and subcortical contributions to long-term memory-guided visuospatial attention. *Cereb Cortex* 28: 2935–2947, 2018. doi:10.1093/cercor/bhx172.

Rosen ML, Stern CE, Michalka SW, Devaney KJ, Somers DC. Influences of long-term memory-guided attention and stimulus-guided attention on visuospatial representations within human intraparietal sulcus. *J Neurosci* 35: 11358–11363, 2015. doi:10.1523/JNEUROSCI.1055-15.2015.

Saproo S, Serences JT. Attention improves transfer of motion information between V1 and MT. *J Neurosci* 34: 3586–3596, 2014. doi:10.1523/JNEUROSCI.3484-13.2014.

Siegel M, Donner TH, Engel AK. Spectral fingerprints of large-scale neuronal interactions. *Nat Rev Neurosci* 13: 121–134, 2012. doi:10.1038/nrn3137.

Sprague TC, Ester EF, Serences JT. Reconstructions of information in visual spatial working memory degrade with memory load. *Curr Biol* 24: 2174–2180, 2014. doi:10.1016/j.cub.2014.07.066.

Sprague TC, Ester EF, Serences JT. Restoring latent visual working memory representations in human cortex. *Neuron* 91: 694–707, 2016. doi:10.1016/j.neuron.2016.07.006.

Sprague TC, Saproo S, Serences JT. Visual attention mitigates information loss in small- and large-scale neural codes. *Trends Cogn Sci* 19: 215–226, 2015. doi:10.1016/j.tics.2015.02.005.

Sprague TC, Serences JT. Attention modulates spatial priority maps in the human occipital, parietal and frontal cortices. *Nat Neurosci* 16: 1879–1887, 2013. doi:10.1038/nn.3574.

Stokes MG, Atherton K, Patai EZ, Nobre AC. Long-term memory prepares neural activity for perception. *Proc Natl Acad Sci USA* 109: E360–E367, 2012. doi:10.1073/pnas.1108555108.

Suchow JW, Brady TF, Fougnie D, Alvarez GA. Modeling visual working memory with the MemToolbox. *J Vis* 13: 9, 2013. doi:10.1167/13.10.9.

Summerfield JJ, Lepsien J, Gitelman DR, Mesulam MM, Nobre AC. Orienting attention based on long-term memory experience. *Neuron* 49: 905–916, 2006. doi:10.1016/j.neuron.2006.01.021.

Sutterer DW, Awh E. Retrieval practice enhances the accessibility but not the quality of memory. *Psychon Bull Rev* 23: 831–841, 2016. doi:10.3758/s13423-015-0937-x.

Sutterer DW, Foster JJ, Adam KCS, Vogel EK, Awh E. Item-specific delay activity demonstrates concurrent storage of multiple active neural representations in working memory. *PLoS Biol* 17: e3000239, 2019. doi:10.1371/journal.pbio.3000239.

Wagner AD, Shannon BJ, Kahn I, Buckner RL. Parietal lobe contributions to episodic memory retrieval. *Trends Cogn Sci* 9: 445–453, 2005. doi:10.1016/j.tics.2005.07.001.

Waldhauser GT, Braun V, Hanslmayr S. Episodic memory retrieval functionally relies on very rapid reactivation of sensory information. *J Neurosci* 36: 251–260, 2016. doi:10.1523/JNEUROSCI.2101-15.2016.

Watrous AJ, Ekstrom AD. The spectro-contextual encoding and retrieval theory of episodic memory. *Front Hum Neurosci* 8: 75, 2014. doi:10.3389/fnhum.2014.00075.

Watrous AJ, Fell J, Ekstrom AD, Axmacher N. More than spikes: common oscillatory mechanisms for content specific neural representations during perception and memory. *Curr Opin Neurobiol* 31: 33–39, 2015. doi:10.1016/j.conb.2014.07.024.

Watrous AJ, Fried I, Ekstrom AD. Behavioral correlates of human hippocampal delta and theta oscillations during navigation. *J Neurophysiol* 105: 1747–1755, 2011. doi:10.1152/jn.00921.2010.

Wheeler ME, Petersen SE, Buckner RL. Memory's echo: vivid remembering reactivates sensory-specific cortex. *Proc Natl Acad Sci USA* 97: 11125–11129, 2000. doi:10.1073/pnas.97.20.11125.

Wilken P, Ma WJ. A detection theory account of change detection. *J Vis* 4: 1120–1135, 2004. doi:10.1167/4.12.11.

Wimber M, Maaß A, Staudigl T, Richardson-Klavehn A, Hanslmayr S. Rapid memory reactivation revealed by oscillatory entrainment. *Curr Biol* 22: 1482–1486, 2012. doi:10.1016/j.cub.2012.05.054.

Worden MS, Foxe JJ, Wang N, Simpson GV. Anticipatory biasing of visuospatial attention indexed by retinotopically specific alpha-band electroencephalography increases over occipital cortex. *J Neurosci* 20: RC63, 2000. doi:10.1523/JNEUROSCI.20-06-j0002.2000.

Xiao X, Dong Q, Gao J, Men W, Poldrack RA, Xue G. Transformed neural pattern reinstatement during episodic memory retrieval. *J Neurosci* 37: 2986–2998, 2017. doi:10.1523/JNEUROSCI.2324-16.2017.

Zhang W, Luck SJ. Discrete fixed-resolution representations in visual working memory. *Nature* 453: 233–235, 2008. doi:10.1038/nature06860.